

## Pressure-induced formation of cubic lutetium hydrides derived from trigonal LuH<sub>3</sub>

Owen Moulding <sup>1,\*</sup>, Samuel Gallego-Parra <sup>2</sup>, Yingzheng Gao,<sup>1</sup> Pierre Toulemonde <sup>1</sup>, Gaston Garbarino,<sup>2</sup> Patricia De Rango <sup>1</sup>, Sébastien Pairis,<sup>1</sup> Pierre Giroux,<sup>1</sup> and Marie-Aude Méasson <sup>1,†</sup>

<sup>1</sup>Institut Néel CNRS/UGA UPR2940, 25 Avenue des Martyrs, 38042 Grenoble, France

<sup>2</sup>European Synchrotron Radiation Facility, 71 Avenue des Martyrs, 38000 Grenoble, France



(Received 13 July 2023; revised 22 September 2023; accepted 14 November 2023; published 4 December 2023)

In recent years, there has been a fervent search for room-temperature superconductivity within the binary hydrides. However, as the number of untested compounds dwindled, it became natural to begin searching within the ternary hydrides. This led to the controversial discovery of room-temperature superconductivity at only 1 GPa in nitrogen-doped lutetium hydride [Dasenbrock-Gammon *et al.*, *Nature (London)* **615**, 244 (2023)] and consequently provided much impetus for the synthesis of nitrogen-based ternary hydrides. Here, we report the synthesis of stable trigonal LuH<sub>3</sub> by hydrogenating pure lutetium which was subsequently pressurized to  $\sim 2$  GPa in a dilute-N<sub>2</sub>/He-rich pressure medium. Raman spectroscopy and x-ray diffraction were used to characterize the structures throughout. After depressurizing, energy-dispersive and wavelength-dispersive x-ray spectroscopies characterized the final compound. Though our compound under pressure exhibits similar structural behavior to the Dasenbrock-Gammon *et al.* sample, we do not observe any nitrogen within the structure of the recovered sample at ambient pressure. We observe two cubic structures under pressure that simultaneously explain the x-ray diffraction and Raman spectra observed: The first corresponds well to  $Fm\bar{3}m$  LuH<sub>2+x</sub>, while the latter is an  $Ia\bar{3}$ -type structure.

DOI: [10.1103/PhysRevB.108.214505](https://doi.org/10.1103/PhysRevB.108.214505)

### I. INTRODUCTION

The holy grail of room-temperature superconductivity has been a long-sought-after quest, ever since the initial predictions of superconductivity in metallic hydrogen by Ashcroft in 1968 [1] and shortly after the publication of BCS theory in 1957 [2,3]. Though not pure hydrogen, many examples of high-temperature superconductivity have been realized in recent years; these have reliably shattered high-critical-temperature (high- $T_c$ ) records with each new discovery. A notable example was SH<sub>3</sub> with a  $T_c$  of 203 K at 155 GPa [4], as it provided tangible promise for the field. Subsequent examples continued to push the threshold with the discovery of superconductivity in YH<sub>9</sub> and LaH<sub>10</sub> at 243 and 260 K, respectively, both at approximately 200 GPa [5–7]. Clearly, these superconducting states require extremely high pressures that few groups are able to reach, and this has been the primary technical challenge to overcome.

This is why the claim of room-temperature superconductivity at 294 K in nitrogen-doped (N-doped) lutetium hydride at such a low pressure of 1 GPa [8] has drawn so much attention. Not only is it a new record  $T_c$  for superconductivity, but also it brings superconductivity into the domain of practicably achievable at near-ambient conditions. Furthermore, the samples are said to be metastable at ambient pressure, which further adds to the wishful properties of such a material. In a short period of time, an impressive number of groups have

already tried to replicate the results, both theoretically and experimentally [9–17], though a corroborative synthesis remains elusive. Even *Nature* has recently published an article entitled “Absence of near-ambient superconductivity in LuH<sub>2+x</sub>N<sub>y</sub>” by Ming *et al.* [14] in direct contention with the original *Nature* publication [8], which goes to show how controversial this discovery has been.

N-doped lutetium hydride represents another step into the domain of ternary compounds following the exhaustive hunt for binary hydride room-temperature superconductors. This new domain is much larger and therefore more daunting to explore; so theoretical predictions are vital to guide experimental works, and they have already yielded several candidate compounds: Li<sub>2</sub>MgH<sub>16</sub> [18,19], YCaH<sub>12</sub> [20,21], ScYH<sub>6</sub> [22], and also the LaH<sub>10</sub>-like clathrate boronitrides La(BN)<sub>5</sub> and Y(BN)<sub>5</sub> [23]. Calculations optimizing superconductivity via doping have also shown that nitrogen from ammonia borane may affect the superconducting properties of LaH<sub>10</sub> [19,24,25]. Experimentally, the most notable confirmed example of a ternary hydride comes from  $Fm\bar{3}m$  (La,Y)H<sub>10</sub> with a superconducting temperature of 253 K at 183 GPa [26]. Beyond this, synthesizing high-quality, high- $T_c$  ternary compounds under extreme pressures remains rare; thus efforts that characterize this phase space in such extreme environments are vital for the field.

In order to synthesize N-doped lutetium hydride, Dasenbrock-Gammon *et al.* [8] and Cai *et al.* [27] used pure lutetium with a H<sub>2</sub>/N<sub>2</sub> gas mixture, whereas other experimental papers started from pure lutetium and NH<sub>4</sub>Cl and CaH<sub>2</sub> precursors [14,15] which decompose to provide the required N<sub>2</sub> and H<sub>2</sub>. Here we choose another process, by first

\*owen.moulding@neel.cnrs.fr

†marie-aude.measson@neel.cnrs.fr

synthesizing pure  $\text{LuH}_3$  and then loading the diamond anvil cell (DAC) with a mixture of dilute  $\text{N}_2$  and helium. We then methodically characterize the obtained compound with Raman spectroscopy and x-ray diffraction (XRD) at each step, and by x-ray energy-dispersive-spectroscopy (EDS) and wavelength-dispersive spectroscopy (WDS) at ambient pressure.

## II. EXPERIMENTAL METHODS

In total we prepared three DACs with thin samples of presynthesized  $\text{LuH}_3$ . Prior to synthesis, polished lutetium metal was characterized by EDS, and oxygen and tantalum were observed in small quantities. The  $\text{LuH}_3$  was then synthesized by hydrogen absorption using the Sievert method by heating for 18 h at  $200^\circ\text{C}$  in 4 MPa of  $\text{H}_2$  gas; further synthesis details are provided in the Supplemental Material (SM), Sec. S1 [28]. All samples came from this synthesis and were distributed among the three DACs. The first DAC (DAC1) was loaded with a mixture of nitrogen and helium, where we estimate that the quantity of  $\text{N}_2$  in the pressure chamber was 4 nmol while the quantity of  $\text{LuH}_3$  was 11 nmol. The other two DACs (DAC2 and DAC3) were loaded with nitrogen: DAC2 was loaded with a gas loader, whereas DAC3 was cryogenically loaded with liquid nitrogen. Among the DACs, only the sample within DAC1 showed structural and chemical transformations under pressure which are discussed in the main text of this paper. The other DACs and further details are discussed in the SM [28]. A ruby ball (for pressure measurement) and a piece of silicon (for optimizing the Raman signal) were also placed inside the pressure chamber. DAC1 was sealed at 1.9 GPa and characterized by Raman spectroscopy and XRD. Though the sample was eventually heated to  $65^\circ\text{C}$  at 1.9 GPa, the main text only presents data prior to heating, as heating had no effect on the structural properties.

The XRD study was performed on the European Synchrotron Radiation Facility (ESRF) ID15B beamline with  $\lambda = 0.411 \text{ \AA}$  at 300 K. Polarized Raman scattering was performed in quasibackscattering geometry at 300 K with an incident laser line at 532 nm from a solid-state laser. The scattered light was analyzed by a single-grating spectrometer and a triple-grating subtractive spectrometer; both were equipped with liquid-nitrogen-cooled CCD detectors. We measured the Raman signal of pure  $\text{LuH}_3$  just before loading in the DAC, after loading at 1.9 GPa, before and after heating, and finally after returning to ambient pressure. After depressurizing, we analyzed the composition of the sample with EDS and WDS while primarily searching for nitrogen.

## III. EXPERIMENTAL RESULTS

### A. Imaging of the sample

The color change from blue at ambient pressure to red at high pressure has been actively discussed in the literature [8,9,15,16]. Images of our sample in DAC1 before (300 K, 1 bar) and after (300 K, 1.9 GPa) loading are presented in Fig. 1. A white light was used to illuminate the sample in reflection and in transmission. Our  $\text{LuH}_3$  sample appears translucent with a red color at 1 bar and seems to

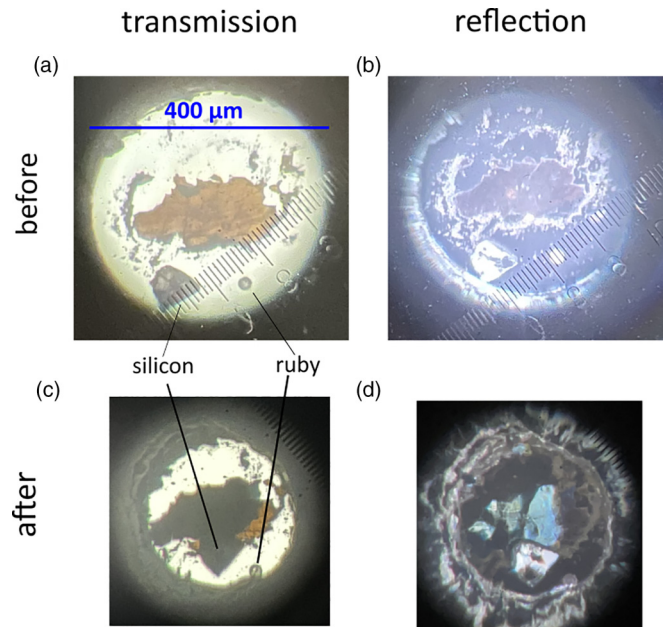


FIG. 1. White-light images of the sample before [(a) and (b)] and after [(c) and (d)] loading at 1.9 GPa. Transmission images are shown in (a) and (c), and reflection images are shown in (b) and (d).

become opaque at high pressure; however, this could be due to the majority of the sample rising up off of the diamond during loading. After loading with the mixture of  $\text{He}/\text{N}_2$  and pressurizing to 1.9 GPa, the surface became reflective and blue. In Fig. 1(c), we can also see a red region which remained flat against the diamond which was also characterized and is discussed in Sec. S2 of the SM [28].

### B. X-ray diffraction

The Rietveld fit of the XRD pattern measured on the trihydride in ambient conditions is shown in Fig. 2(a), and we determine the structure to be trigonal  $P\bar{3}c1$  with lattice parameters of  $a = 6.173(1) \text{ \AA}$  and  $c = 6.424(1) \text{ \AA}$ . The lanthanide trihydrides tend to adopt either this trigonal structure or a hexagonal  $P6_3/mmc$  structure (the higher-symmetry parent group) [29]. Previously, Tkacz and Palasyuk [30] determined that  $\text{LuH}_3$  is hexagonal with  $a = 3.57 \text{ \AA}$  and  $c = 6.41 \text{ \AA}$  at ambient conditions. However, previous measurements had already shown that the structure is trigonal with lattice parameters of  $a = 6.16 \text{ \AA}$  and  $c = 6.44 \text{ \AA}$  [31], which are similar to our values. Furthermore, recent calculations by Dangić *et al.* predict that the trigonal structure should be more stable than the hexagonal structure in this pressure range [32]. Finally, the hexagonal structure would also be inconsistent with the Raman spectra we measured due to having too few excitations, as shown in Table SIV of Sec. S5 in the SM [28]. Overall we conclude that our starting  $\text{LuH}_3$  adopts a trigonal  $P\bar{3}c1$  structure in ambient conditions.

With regard to impurities within our sample, from the Rietveld fit we determine that the sample is primarily  $\text{LuH}_3$  at 96.9(1)%, and the rest was identified to be  $\text{Lu}_2\text{O}_3$ . The  $\text{Lu}_2\text{O}_3$  is likely to originate from deposits on the lutetium surface that were not removed by polishing before hydrogenation. The

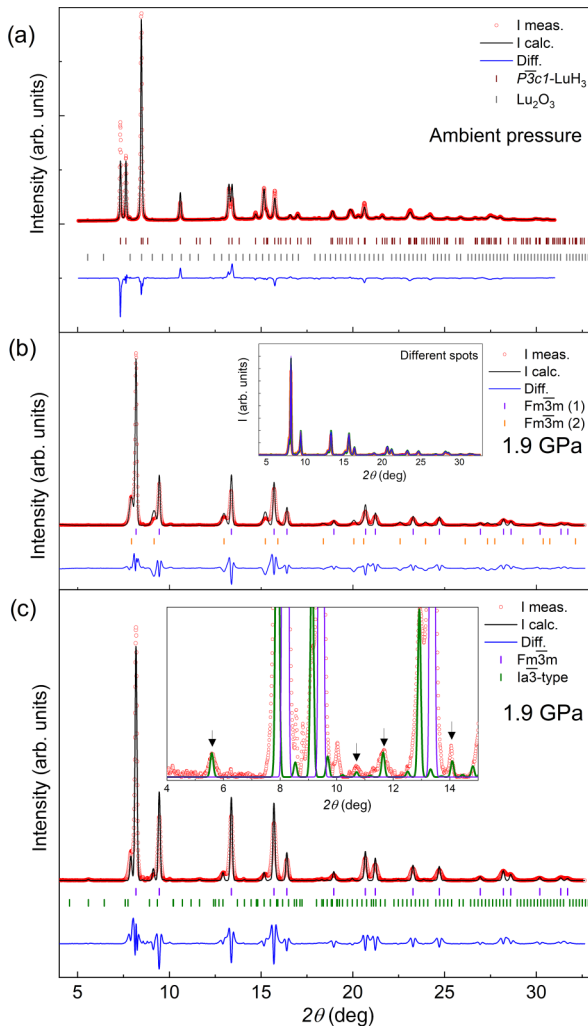


FIG. 2. Rietveld refinements of the patterns measured at the ESRF (beamline ID15B,  $\lambda = 0.411$  Å) at 300 K. (a) The trigonal  $\text{LuH}_3$  sample at ambient pressure. (b) The high-pressure compound at 1.9 GPa and fitted with two  $Fm\bar{3}m$  structures, structures 1 and 2. Inset: patterns measured on five different spots. (c) The high-pressure compound at 1.9 GPa and fitted with one  $Fm\bar{3}m$  structure and one  $Ia\bar{3}$ -type structure. Inset: zoom of some of the weak reflections fitted by the  $Ia\bar{3}$ -type structure (cf. arrows). Diff., difference between measured and calculated values.

space group of  $\text{Lu}_2\text{O}_3$  is  $Ia\bar{3}$ , and the refined lattice parameter is  $10.380(8)$  Å in agreement with the literature [33,34]. We also show that the percentage of  $\text{Lu}_2\text{O}_3$  stays constant for 6 months with the sample exposed directly to air (Sec. S2 of the SM [28]); so the sample is stable with respect to oxidation within this time scale. The EDS measurements showed that a small quantity of tantalum was present in the starting lutetium; however, there are no signatures of tantalum or tantalum hydride in the XRD spectra.

XRD patterns from the loaded sample at 1.9 GPa are shown in Fig. 2(b). They were measured in five different spots with sizes of  $4 \times 3$   $\mu\text{m}$  and separated by 20  $\mu\text{m}$  in a cross shape. The results on the different spots are remarkably similar and indicate that the sample is homogeneous in this region [see inset of Fig. 2(b)]. By comparing the XRD

patterns, the transformation to a new phase is clear. In their paper, Dasenbrock-Gammon *et al.* determine the synthesized ambient pressure sample to consist of two distinct  $Fm\bar{3}m$  phases [8]: The majority  $\text{LuH}_{3-\delta}\text{N}_\epsilon$  “A” phase (92.25% of the sample) has a lattice parameter of  $a_A = 5.0298(4)$  Å, while the lattice parameter of the minority  $\text{LuN}_{1-\delta}\text{H}_\epsilon$  “B” phase (7.29%) is  $a_B = 4.7529(9)$  Å [8]. Under pressure at 1.9 GPa, we obtain similar XRD patterns that can be reasonably well described by two  $Fm\bar{3}m$  phases. Our majority phase ( $\approx 60\%$ ) has a lattice parameter of  $a_1 = 4.990(6)$  Å, while our minority phase ( $\approx 40\%$ ) has a lattice parameter of  $a_2 = 5.145(2)$  Å. We note that our majority phase is the one with the smaller lattice parameter, but more disconcertingly, we notice that the lattice parameters of both of our phases are larger than those of Dasenbrock-Gammon *et al.* despite our compound being under pressure. A tempting explanation might rely on the synthesis process, which, starting from pure  $\text{LuH}_3$ , would tend to produce compounds with higher hydrogen content that are closer to the trihydride with an expanded lattice.

Interestingly, after pressurization there are some small reflections that cannot be described by the refinement using two  $Fm\bar{3}m$  phases. Moreover, there is a clear inconsistency between the two  $Fm\bar{3}m$  phases and the Raman spectra, as shall be discussed in more detail later. This leads us to reconsider the structural composition, and our analysis is in favor of one  $Fm\bar{3}m$  structure and one  $Ia\bar{3}$  structure.

Indeed, Fig. 2(c) shows that the small reflections can be better explained by refining the XRD data at 1.9 GPa with one  $Fm\bar{3}m$  structure and one  $Ia\bar{3}$  structure. From this refinement, we obtained lattice parameters of  $4.99(3)$  and  $10.329(3)$  Å for the  $Fm\bar{3}m$  and  $Ia\bar{3}$  structures, respectively. The lattice parameter of the  $Fm\bar{3}m$  structure remains the same within error as that of the previous refinement using two  $Fm\bar{3}m$  structures. Here we exclude the presence of  $Fm\bar{3}m$   $\text{LuH}_3$ , since this phase was only observed previously above 12 GPa [30], far beyond our measured pressure range. However, other  $Fm\bar{3}m$  compounds remain possible and shall be discussed later.

Regarding the  $Ia\bar{3}$  phase, we notice that it is similar to the second  $Fm\bar{3}m$  structure but with an approximate doubling of the lattice parameter ( $2a_2$ , eight times the volume) and a slightly lower symmetry. Though the  $Ia\bar{3}$ -type structure is similar to the  $Fm\bar{3}m$  structure, the lutetium atoms occupy different Wyckoff positions within the lattice: namely, the  $8b$  and  $24d$  sites. The  $8b$  site is highly symmetric,  $(1/4, 1/4, 1/4)$ , while the  $24d$  site is described by  $(x, 0, 1/4)$ , where  $x$  was determined to be approximately  $0.975(8)$ . This small difference from unity is indicative of a slight distortion in the lutetium sublattice relative to the global cubic symmetry. The occupation of the  $24d$  site also has ramifications for the Raman activity as it provides eight additional phonons, whereas the  $8b$  site does not provide any. This shall be discussed further in later sections.

Even though the  $Ia\bar{3}$  phase is reminiscent of  $\text{Lu}_2\text{O}_3$ , we state that it is not the same compound. Firstly, the lattice parameter is smaller than the value of  $10.357$  Å for  $\text{Lu}_2\text{O}_3$  at 1.9 GPa, which was determined from the volume dependence of Ref. [34]. Secondly, since the  $Ia\bar{3}$  compound is recoverable (though metastable on the time scale of days as shown in Sec. S3 of the SM), we determine that the ambient pressure lattice parameter is  $10.41(1)$  Å (see Sec. S3 of the SM),

TABLE I. The total number of optical infrared-active (IR-active) and Raman-active (R-active) modes for the given space groups with the occupied Wyckoff positions stated for various compounds.

Space group	Lu	H <sup>1</sup>	H <sup>2</sup>	H <sup>3</sup>	IR-active	R-active
$Fm\bar{3}m$ (LuH <sub>3</sub> [12])	4a	8c	4b		2T <sub>1u</sub>	1T <sub>2g</sub>
$Fm\bar{3}m$ (LuH <sub>2+x</sub> )	4a	8c	4b		2T <sub>1u</sub>	1T <sub>2g</sub>
$Fm\bar{3}m$ (LuH <sub>2</sub> [12])	4a	8c			1T <sub>1u</sub>	1T <sub>2g</sub>
$P\bar{3}c1$ (YH <sub>3</sub> [36])	6f	2a	4d	12g	6A <sub>2u</sub> + 11E <sub>u</sub>	5A <sub>1g</sub> + 12E <sub>g</sub>
Space group	Lu <sup>1</sup>	Lu <sup>2</sup>	H <sup>1</sup>	H <sup>2</sup>	IR-active	R-active
$Ia\bar{3}$ ( $Ia\bar{3}$ -type)	8b	24d			7T <sub>u</sub>	1A <sub>g</sub> + 2E <sub>g</sub> + 5T <sub>g</sub>

which is larger than the ambient pressure value for Lu<sub>2</sub>O<sub>3</sub> of 10.38 Å [34]. Together, these lattice parameters at ambient and high pressure indicate that the  $Ia\bar{3}$  phase has a larger compressibility than Lu<sub>2</sub>O<sub>3</sub>, which further distinguishes them as separate compounds. Finally, the Raman spectrum, as shown in the next section, does not contain the expected main Raman mode of Lu<sub>2</sub>O<sub>3</sub>. Therefore we conclude that the high-pressure sample of DAC1 does not contain two  $Fm\bar{3}m$  phases, but in fact one  $Fm\bar{3}m$  phase and one  $Ia\bar{3}$  phase that we shall label as an  $Ia\bar{3}$ -type phase henceforth.

### C. Raman spectroscopy

We first recall the nature of the  $\Gamma$ -point phonons expected in the various space groups under consideration (see Sec. S5 of the SM for more space groups [28]). From the literature on LuH<sub>3</sub> (and YH<sub>3</sub>), the crystal structure could correspond to  $Fm\bar{3}m$  or  $P\bar{3}c1$  [29,35,36]. We expect a total of  $5A_{1g} \oplus 12E_g$  Raman-active phonon modes in the trigonal  $P\bar{3}c1$  phase and a single Raman-active  $T_{2g}$  mode in the  $Fm\bar{3}m$  structure, as stated in Table I. The  $T_{2g}$  mode is associated with the displacement of the hydrogen atoms occupying the 8c Wyckoff sites and is also expected to appear in  $Fm\bar{3}m$  LuH<sub>2</sub> and  $Fm\bar{3}m$  LuH<sub>2+x</sub>. Here we note that the  $Fm\bar{3}m$  LuH<sub>2</sub> and LuH<sub>3</sub> are related by the partial and continuous occupation of the octahedral 4b sites, which results in the formation of LuH<sub>2+x</sub>. Spectroscopically, and as shown in Table I,  $Fm\bar{3}m$  LuH<sub>3</sub> and LuH<sub>2+x</sub> behave very similarly, while  $Fm\bar{3}m$  LuH<sub>2</sub> lacks a  $T_{1u}$  mode since the 4b site is completely unoccupied.

Wide-range Raman spectra on the ambient pressure trigonal LuH<sub>3</sub> and the high-pressure sample are shown in Fig. 3(a). For the ambient pressure trigonal phase, we observe at least 12 features that are marked by black arrows. This is close to the 17 phonon modes expected for the trigonal  $P\bar{3}c1$  structure and supports our XRD analysis. Importantly, the number of modes far exceeds the four phonon modes predicted for the alternative hexagonal  $P6_3/mmc$  structure (see Sec. S5 of the SM); so we can conclusively exclude it as a viable structure. As we increase the pressure, we clearly observe the disappearance of all the phonons observed associated with the trigonal phase, which is indicative of a structural transition. We also observe a large increase in the background by a factor of  $\sim 10$ , though we cannot conclude whether it is intrinsic or due to the angle of the sample as compared with the diamond. Most notably, we observe two peaks at high pressure that consistently appear at approximately 1240 and 260 cm<sup>-1</sup> which were not present at ambient pressure.

At energies below 260 cm<sup>-1</sup> we observe other features, most notably three weak excitations at 202, 164, and 128 cm<sup>-1</sup>. As shown in Fig. 3(b), these are similar to not only those observed by Dasenbrock-Gammon *et al.* [8] but also those observed by Xing *et al.* [15], who ascribed them to vibrational modes of  $Fm\bar{3}m$  compounds. However, the number of Raman modes is inconsistent with two  $Fm\bar{3}m$  structures, as we only expect one  $T_{2g}$  mode for each phase.

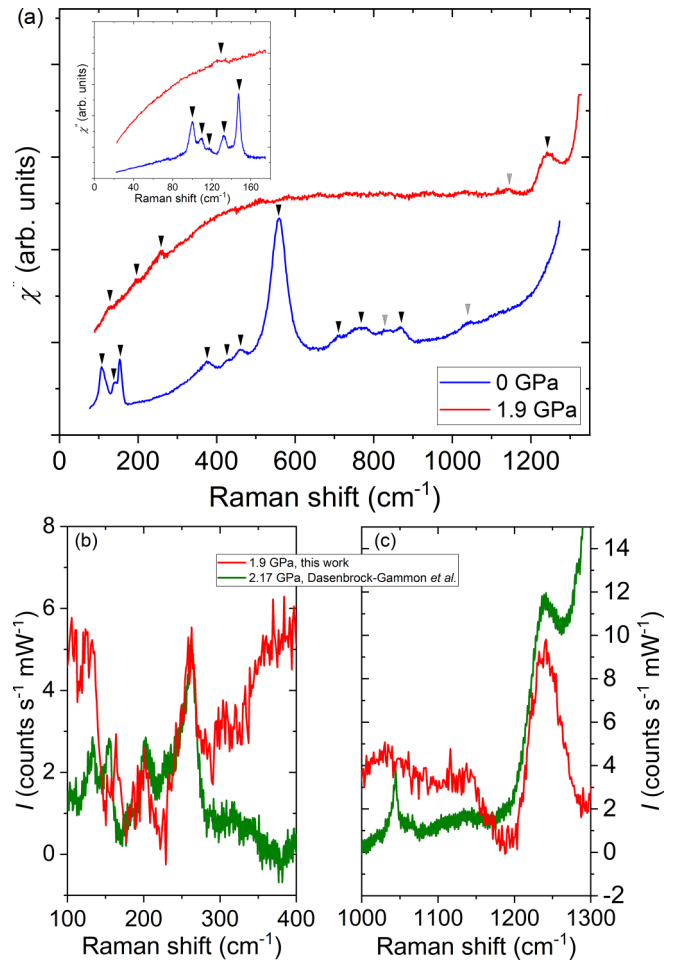


FIG. 3. (a) Raman spectra of trigonal LuH<sub>3</sub> at ambient pressure (blue) and a high-pressure sample at 1.9 GPa (red). The inset shows low-energy triple-stage data. (b) and (c) show our data scaled on the Dasenbrock-Gammon *et al.* data at  $\sim 2$  GPa [8]. We scale on the peak at 260 cm<sup>-1</sup> after a background correction which aids the comparison. The scaling in (b) is the same as in (c).

Furthermore, we do not expect the lower-symmetry Wyckoff sites (e.g.,  $24e$ ,  $32f$ , etc.) to become occupied since hydrogen concentrations above three H atoms per Lu atom have not been observed at these pressures. Herein lies the contradiction with these previous analyses: Two  $Fm\bar{3}m$  structures cannot explain the number of phonon modes observed here and previously [8,15]. On the other hand, a distortion to a  $Ia\bar{3}$ -type phase with lutetium atoms on the  $24d$  Wyckoff sites provides  $1A_g \oplus 2E_g \oplus 5T_g$  phonon modes, and since the lutetium atoms are heavy, these phonon modes would be at low energy. Thus the  $Ia\bar{3}$ -type phase could provide the required modes at low energy that were observed by us and others [8,15].

#### IV. DISCUSSION

To summarize the results, from the XRD we have observed a biphasic mixture of cubic  $Fm\bar{3}m$  and cubic  $Ia\bar{3}$  by accounting for the numerous weak reflections. These weak reflections are not described by two  $Fm\bar{3}m$  structures. From the Raman spectroscopy, we observe one strong mode at  $1240\text{ cm}^{-1}$  and several weak modes at and below  $260\text{ cm}^{-1}$ . The number of modes cannot be explained by two  $Fm\bar{3}m$  structures, whereas the  $Ia\bar{3}$  structure can in principle provide many modes at low energy. As clearly stated by Hilleke *et al.* [17], from the XRD results the identified sublattices of lutetium atoms (fcc for an  $Fm\bar{3}m$  structure and bcc for an  $Ia\bar{3}$  structure) provides a constraint about which we should search but it does not necessarily describe the entire structure. Now we shall discuss the possible origin of these structures, and whether or not known compounds can explain the data.

Firstly, we shall address the contaminants which include  $\text{Lu}_2\text{O}_3$ , pure tantalum,  $\text{TaH}_{1-x}$ , and the van der Waals solid  $\text{He}(\text{N}_2)_{11}$  [37]. This last compound forms beyond the pressure range of interest (above 9 GPa), and the stoichiometry of the pressure medium is vastly different from that of the compound; so we do not think that it is present. We have already shown that the  $\text{Lu}_2\text{O}_3$  impurities are minor in our XRD pattern at ambient pressure ( $\approx 3\%$ ); so we do not expect a large effect from their presence. Furthermore, we do not see any Raman signature of this phase. Indeed, the most intense Raman-active mode of  $\text{Lu}_2\text{O}_3$  is observed at  $390\text{ cm}^{-1}$  at ambient pressure (shown in Sec. S3 of the SM [28]) and hardens slightly up to  $400\text{ cm}^{-1}$  at 2 GPa [34]. However, there is no indication of this mode in any of the locations measured. Therefore we eliminate  $\text{Lu}_2\text{O}_3$  as being responsible for the XRD pattern and Raman-active modes, at either ambient or high pressure. Though the quantity is small ( $\approx 1\%$ ), pure tantalum and  $\text{TaH}_{1-x}$  could potentially be present. Pure tantalum forms an  $Im\bar{3}m$  structure [38], whereas  $\text{TaH}_{1-x}$  forms an  $I\bar{4}m2$  structure [39]. Neither structure can explain the XRD reflections, and so we also eliminate pure tantalum and  $\text{TaH}_{1-x}$  from consideration.

One should also consider intercalation effects from the pressure medium itself. Previous measurements have shown that helium can occupy interstitial voids and change the structural properties of materials under pressure [40–44]. This effect seems confined to network-forming structures [40] or to materials possessing large voids such as single-wall carbon nanotubes [41,42], fullerenes [43], or clathrates [44]. However, neither trigonal,  $Fm\bar{3}m$ , nor  $Ia\bar{3}$ -type phases form these

types of structures, and so we do not expect such helium intercalation; see Sec. S2 of the SM for further discussion. Nor would we expect an intercalation effect from  $\text{N}_2$  molecules due to their much larger size.

We will now compare our XRD and Raman results with the known phases in the Lu-H-N landscape at room temperature and  $\sim 2$  GPa. These consist of pure  $\text{N}_2$  phases,  $Fm\bar{3}m$  ammonia ( $\text{NH}_3$ ) [45,46], fcc rock-salt LuN (RS-LuN; NaCl-type  $B_1$ ,  $Fm\bar{3}m$ ), fcc zinc-blende LuN (ZB-LuN; ZnS-type  $B_3$ ,  $F\bar{4}3m$ ), hexagonal  $\text{LuH}_8$  ( $P6_3/mmc$ ), and fcc  $\text{LuH}_2$  (CaF $_2$ -type,  $Fm\bar{3}m$ ).

At room temperature and 2 GPa, pure  $\text{N}_2$  may form either a fluid or a solid  $\beta$  phase. The  $\beta$  phase crystallizes in a  $P6_3/mmc$  structure [47,48], and a single mode is expected at  $\sim 2330\text{ cm}^{-1}$ , which we observe as a narrow peak in this range of energy.  $\text{N}_2$  gas has not only a similar vibron mode at high energy but also other peaks at low energy below  $150\text{ cm}^{-1}$  [49]. Some of the modes that we measured might originate from  $\text{N}_2$  gas, but not the ones at  $195$  and  $166\text{ cm}^{-1}$  or our dominant modes at  $1240$  or  $260\text{ cm}^{-1}$ .

Ammonia could in principle form if hydrogen liberated from the trigonal  $\text{LuH}_3$  lattice reacted with nitrogen instead of being replaced by it. At 2 GPa and ambient temperature, ammonia is expected to form a  $Fm\bar{3}m$  structure which should only possess one Raman-active mode [46,50]. Ammonia is unlikely to be detected by XRD due to the weak signal from the light atoms contrasted against the large contribution from the massive lutetium atoms; therefore it is unlikely that any of the refined cubic phases could originate from it. Raman scattering under pressure shows that only modes at energies higher than  $3100\text{ cm}^{-1}$  are observed in this phase [46]. So we exclude ammonia from being responsible for the Raman modes we measure at 1.9 GPa.

The primary potential nitride compound is  $Fm\bar{3}m$  RS-LuN, which has a lattice parameter of  $a = 4.7563(4)\text{ \AA}$  at ambient conditions [51]. Therefore this cannot explain either of the two cubic phases observed by XRD, as the lattice parameter will only continue to shrink under pressure and it is already smaller than both of the lattice parameters measured. Furthermore, RS-LuN is in principle Raman inactive since only the  $4a$  and  $4b$  Wyckoff sites are occupied. Despite this, a strong excitation was observed previously at  $582\text{ cm}^{-1}$  and was ascribed to strong disorder [52]. Regardless, we do not observe this mode. We also note that the synthesis of RS-LuN is challenging and previously required heating pure lutetium and nitrogen at  $1600\text{ }^\circ\text{C}$  [51]. Thus, since we have not laser-heated our sample, we do not expect the formation of this compound. The EDS and WDS also support the idea that RS-LuN did not form (see Sec. S4 of the SM) since this would result in a clear signature from nitrogen as this compound is stable at ambient pressure. On the other hand, the  $F\bar{4}3m$  ZB-LuN isomorph has only been predicted to form at pressures above 260 GPa [53,54]. Experimentally, the RS-LuN structure was shown to form preferentially when synthesized at 30 GPa and 2000 K [55]; that is to say, in far more extreme conditions than were attained here and in other papers, the ZB-LuN structure could not be formed, and so we do not consider it viable from here on.

Since we do not observe any signatures of trigonal  $\text{LuH}_3$  and we do not expect cubic  $\text{LuH}_3$  at 2 GPa based on its

predicted and observed stability [12,17,29,30,56], it is likely that other lutetium hydrides have formed via the decomposition of the trigonal LuH<sub>3</sub>. Firstly, hexagonal  $P6_3/mmc$  LuH<sub>3</sub> compounds ( $0 \leq \delta \leq 0.2$ ) form for low hydrogen concentrations [57–60]. At most, these hexagonal compounds could contribute four Raman-active phonons which would help explain the low-energy modes. However, our attempts to reproduce the XRD patterns with any hexagonal structure at high pressure failed. We note that, in the recovered sample at ambient pressure, we were able to identify this phase (see Sec. S3 of the SM).

The other primary lutetium hydride is  $Fm\bar{3}m$  LuH<sub>2</sub>, or the similar compound  $Fm\bar{3}m$  LuH<sub>2+x</sub> with partially occupied 4b sites. The lattice parameter of  $Fm\bar{3}m$  LuH<sub>2</sub> is reported to be  $a = 5.033$  Å at ambient conditions [14,61,62], which is also consistent with LuH<sub>2+x</sub>. These phases can therefore explain the XRD pattern of the refined  $Fm\bar{3}m$  phase. With regard to the Raman activity, we expect one Raman-active  $T_{2g}$  mode which was calculated to be between 960 and 1170 cm<sup>-1</sup> at ambient pressure [32]. This would be consistent with the mode measured at 1240 cm<sup>-1</sup> at 1.9 GPa. To explain our mode measured at 260 cm<sup>-1</sup>, we note that an infrared-active  $T_{1u}$  mode is predicted to appear at 250 cm<sup>-1</sup> in  $Fm\bar{3}m$  LuH<sub>3</sub> [12,32]. Since  $Fm\bar{3}m$  LuH<sub>3</sub> and LuH<sub>2+x</sub> are structurally similar, one would expect that they share the predicted mode. LuH<sub>2</sub> lacks this mode [32]. Thus, provided that the  $T_{1u}$  mode becomes Raman active, potentially by disorder, our excitations at 1240 and 260 cm<sup>-1</sup> could provide evidence for the presence of  $Fm\bar{3}m$  LuH<sub>2+x</sub>. Furthermore, the blue color observed in Fig. 1(d) would also be consistent with the formation of  $Fm\bar{3}m$  LuH<sub>2+x</sub>, as it is also predicted to be blue [63]. In summary,  $Fm\bar{3}m$  LuH<sub>2+x</sub> is consistent with both the Raman spectra and XRD patterns we measured. However, it is clear that this phase alone cannot explain the low-energy modes since no other Raman-active modes exist, and the only other predicted  $T_{1u}$  mode is at high energy (above 1000 cm<sup>-1</sup> [12,32]).

Though we identify the  $Fm\bar{3}m$  structure as LuH<sub>2+x</sub>, we still cannot explain the remaining Raman modes or the  $Ia\bar{3}$  phase identified by XRD results with known phases. So, we shall discuss now the potential formation of the N-doped lutetium hydride compound. In Sec. S3 of the SM [28], we show that once the pressure is released, the sample is metastable but still contains the  $Fm\bar{3}m$  and  $Ia\bar{3}$  phases. Most importantly, the recovered sample does not contain nitrogen as shown by both the EDS and WDS in Sec. S4 of the SM [28].

In fact, metal nitrides are generally challenging to form due to the significant activation barrier of the nonpolar, triple-bonded nitrogen atoms (bond energy 941 kJ/mol) [64]. However once synthesized, these nitrides tend to have refractory properties and are thermally and chemically stable [64]. Previously, Dierkes *et al.* synthesized LuN by nitrating LuH<sub>3</sub> [65], which is the closest analogy to the desired reaction for this work. They note that nitridation does not start below 800 °C and even then the uptake of nitrogen is slow until above 900 °C [65]; they also note that LuH<sub>3</sub> begins to decompose by releasing hydrogen above 300 °C. Perhaps, heating within this window under pressure would favor the formation of N-doped lutetium hydride. Cai *et al.* performed a laser-heating synthesis at 1800 °C with pure lutetium and N<sub>2</sub>/H<sub>2</sub>

pressure medium, which formed a mixture of LuH<sub>2</sub> and LuH<sub>3</sub> with no observable nitride compounds [27]. Theoretically, it has been reliably noted that there are no thermodynamically stable ternary Lu-H-N compounds: only metastable ones at best [10,12,17,56,66]. Furthermore, we prepared two pressure cells with pure nitrogen pressure media, and we observed no change in the trigonal LuH<sub>3</sub> structure upon heating to 65 °C at 2 GPa followed by pressurizing to 12 GPa. This indicates that nitrogen has a limited effect on the sample; further details are provided in Secs. S2 and S3 of the SM. So based on all of this, it would seem that the synthesis, as stated in the *Nature* paper [8], of heating the DAC for 24 h at 65 °C and 2 GPa to form N-doped lutetium hydride would be unlikely to occur.

Fortunately, with the publication of Dias's patent, we can gain insight into an alternative synthesis method [67]. According to Fig. 1 of the patent, this patentable synthesis involves heating lutetium metal in a reaction chamber with hydrogen and nitrogen gas at 4–10 MPa and 200–400 °C for 12–24 h before being pressurized to 3–20 kbar in a DAC [67]; this is rather different from the synthesis stated in the *Nature* paper [8]. Despite this, our synthesis by preforming LuH<sub>3</sub> at 200 °C with 4 MPa of H<sub>2</sub> prior to loading is providentially similar, though we did not include nitrogen in this part of the synthesis. This patentable synthesis is also very similar to the work of Dierkes *et al.* [65], though they did not heat with the two gases together in the reaction chamber at the same time. This combined with our work strongly suggests that heating the pure lutetium metal in a hydrogen and nitrogen atmosphere at high temperatures (above 200 °C) is vital for the formation of the N-doped lutetium hydride.

Overall, these considerations for the nitridation of lutetium hydride are also relevant for the partial or complete nitridation of other rare-earth hydrides and for the formation of other nitrogen compounds. Pragmatically, the successes of the rare-earth elements in producing high-temperature superconductors and the prevalence of ammonia borane syntheses have already shifted the direction of research, as evidenced by the predictions of nitrogen doping of rare-earth compounds [19,24,25] or simply rare-earth nitrogen compounds such as the clathrate boronitrides La(BN)<sub>5</sub> and Y(BN)<sub>5</sub> [23]. As a result, the incorporation of nitrogen into rare-earth hydrides is a logical route of inquiry for future experimental works where the challenges of nitrogen chemistry will have to be taken into account.

In our case, we cannot conclusively say that we did or did not form N-doped LuH<sub>3</sub> at 1.9 GPa, as it could have decomposed and ejected the nitrogen prior to the EDS and WDS measurements; however, it seems unlikely given the arguments discussed. What is clear is that at 1.9 GPa, we formed a compound that is similar to that described by Dasenbrock-Gammon *et al.* [8], but ours was metastable and eventually decayed at ambient conditions. What is also clear is that the contradictory nature of observing many Raman-active phonons with two  $Fm\bar{3}m$  lutetium lattices was an overlooked problem. Overall, the question then becomes, What is the origin of the  $Ia\bar{3}$ -type phase?

To explain the origin of the  $Ia\bar{3}$ -type phase, we speculate that this structure arises from a charge-density-wave (CDW) distortion of a pure lutetium hydride compound. Previous work on the chemically similar ScH<sub>3</sub> and YH<sub>3</sub> shows that

there is an intermediate region between the ambient pressure trigonal or hexagonal structure and the high-pressure cubic phase [68–70]. Theoretical work on  $\text{YH}_3$  predicts that a Peierls-distorted  $C2/m$  structure forms within this intermediate phase that continues to possess a close approximation of a cubic sublattice [69]. Unfortunately, we tried an XRD refinement of the proposed  $C2/m$  structure without success, but this does not eliminate the possibility that this mechanism gives rise to other distorted structures. A similar intermediate phase was also observed in  $\text{ScH}_3$  between 25 and 46 GPa [70], whereas this phase was observed in  $\text{YH}_3$  between 9 and 24 GPa [68]. Since lutetium is chemically similar to scandium and yttrium, one could hypothesize that a similar intermediate Peierls-distorted/CDW phase could arise in our lutetium hydride compound. The CDW then provides a mechanism to form our  $Ia\bar{3}$ -type phase, which is then a distortion of a higher-symmetry phase: perhaps  $Fm\bar{3}m$  due to the already existing similarities. Furthermore, the pressure range of the intermediate phase seems to decrease with increasing atom size; that is to say, this intermediate phase could then coincide with our measured pressure range. It is also worth noting that a strong change in the optical gap has been observed within the CDW phase in both  $\text{YH}_3$  and  $\text{ScH}_3$  [68,70]. As such, the observation of poor-metal behavior and upturns in the resistivity in previous measurements on lutetium hydrides [14,16,71,72] could then be evidence of a CDW phase as the gap opens. Overall, a CDW phase driving the formation of the  $Ia\bar{3}$ -type phase could then simultaneously explain some of the electrical properties observed, the cubic lattice of lutetium atoms, and the forest of Raman-active modes observed at low energy without invoking the synthesis of a ternary compound.

## V. CONCLUSION

We obtain a biphasic sample which presents structural similarities to the sample of Dasenbrock-Gammon *et al.* [8] by starting from pure trigonal  $\text{LuH}_3$  loaded in a DAC at

1.9 GPa with a mixture of  $\text{N}_2/\text{He}$ . From x-ray diffraction, we clearly see a structural transformation from the initial trigonal phase to a mixture of cubic phases under pressure. Similarly, with Raman spectroscopy we observe the loss of the modes associated with the trigonal structure and see the appearance of a strong mode at  $1240\text{ cm}^{-1}$  that we associate with the  $T_{2g}$  Raman-active mode of a cubic  $Fm\bar{3}m$  structure. However, we (and others) observe more excitations than are possible for two  $Fm\bar{3}m$  cubic structures. Overall we believe that it is unlikely that these excitations come from impurity phases since either they are not visible in XRD, they are chemically unlikely to form, or simply their excitations do not occur in the energy range. Thus we conclude that our sample is a biphasic mixture of  $Fm\bar{3}m\text{ LuH}_{2+x}$  and an  $Ia\bar{3}$ -type structure, also composed of lutetium and hydrogen, which together may describe the XRD patterns and Raman spectra. We postulate that the  $Ia\bar{3}$ -type structure is a distortion of a higher-symmetry structure and could originate from a CDW phase. However, further theoretical work will be needed to support the origin and stability of this phase. More broadly, our discussion of nitrogen chemistry will aid future works in experimentally finding ternary compound superconductors.

## ACKNOWLEDGMENTS

This work is supported by the European Research Council (ERC) under the European Union's Horizon 2020 research and innovation program (Grant Agreement No. 865826). This work has received funding from the Agence Nationale de la Recherche under the project SADAHPT. We thank Abdellali Hadj-Azzem and Elise Pachoud for lutetium preparation and Céline Goujon for help in the preparation of the laboratory high-pressure XRD setup. We thank Laetitia Laversenne for fruitful discussions and Eva Zurek for stimulating exchanges of information.

The authors declare no competing interests.

- 
- [1] N. W. Ashcroft, Metallic hydrogen: A high-temperature superconductor? *Phys. Rev. Lett.* **21**, 1748 (1968).
  - [2] J. Bardeen, L. N. Cooper, and J. R. Schrieffer, Theory of superconductivity, *Phys. Rev.* **108**, 1175 (1957).
  - [3] J. Bardeen, L. N. Cooper, and J. R. Schrieffer, Microscopic theory of superconductivity, *Phys. Rev.* **106**, 162 (1957).
  - [4] A. P. Drozdov, M. I. Erements, I. A. Troyan, V. Ksenofontov, and S. I. Shylin, Conventional superconductivity at 203 kelvin at high pressures in the sulfur hydride system, *Nature (London)* **525**, 73 (2015).
  - [5] P. Kong, V. S. Minkov, M. A. Kuzovnikov, A. P. Drozdov, S. P. Besedin, S. Mozaffari, L. Balicas, F. F. Balakirev, V. B. Prakapenka, S. Chariton, D. A. Knyazev, E. Greenberg, and M. I. Erements, Superconductivity up to 243 K in the yttrium-hydrogen system under high pressure, *Nat. Commun.* **12**, 5075 (2021).
  - [6] M. Somayazulu, M. Ahart, A. K. Mishra, Z. M. Geballe, M. Baldini, Y. Meng, V. V. Struzhkin, and R. J. Hemley, Evidence for superconductivity above 260 K in lanthanum superhydride at megabar pressures, *Phys. Rev. Lett.* **122**, 027001 (2019).
  - [7] A. P. Drozdov, P. P. Kong, V. S. Minkov, S. P. Besedin, M. A. Kuzovnikov, S. Mozaffari, L. Balicas, F. F. Balakirev, D. E. Graf, V. B. Prakapenka, E. Greenberg, D. A. Knyazev, M. Tkacz, and M. I. Erements, Superconductivity at 250 K in lanthanum hydride under high pressures, *Nature (London)* **569**, 528 (2019).
  - [8] N. Dasenbrock-Gammon, E. Snider, R. McBride, H. Pasan, D. Durkee, N. Khalvashi-Sutter, S. Munasinghe, S. E. Dissanayake, K. V. Lawler, A. Salamat, and R. P. Dias, RETRACTED ARTICLE: Evidence of near-ambient superconductivity in a N-doped lutetium hydride, *Nature (London)* **615**, 244 (2023).
  - [9] P. Shan, N. Wang, X. Zheng, Q. Qiu, Y. Peng, and J. Cheng, Pressure-induced color change in the lutetium dihydride  $\text{LuH}_2$ , *Chin. Phys. Lett.* **40**, 046101 (2023).
  - [10] Z. Huo, D. Duan, T. Ma, Z. Zhang, Q. Jiang, D. An, H. Song, F. Tian, and T. Cui, First-principles study on the conventional superconductivity of N-doped  $fcc\text{-LuH}_3$ , *Matter Radiat. Extremes* **8**, 038402 (2023).

- [11] Z. Li, X. He, C. Zhang, K. Lu, B. Min, J. Zhang, S. Zhang, J. Zhao, L. Shi, Y. Peng, S. Feng, Z. Deng, J. Song, Q. Liu, X. Wang, R. Yu, L. Wang, Y. Li, J. D. Bass, V. Prakapenka *et al.*, Superconductivity above 70 K observed in lutetium polyhydrides, *Sci. China: Phys., Mech. Astron.* **66**, 267411 (2023).
- [12] Y. Sun, F. Zhang, S. Wu, V. Antropov, and K.-M. Ho, Effect of nitrogen doping and pressure on the stability of  $\text{LuH}_3$ , *Phys. Rev. B* **108**, L020101 (2023).
- [13] F. Xie, T. Lu, Z. Yu, Y. Wang, Z. Wang, S. Meng, and M. Liu, Lu–H–N phase diagram from first-principles calculations, *Chin. Phys. Lett.* **40**, 057401 (2023).
- [14] X. Ming, Y.-J. Zhang, X. Zhu, Q. Li, C. He, Y. Liu, T. Huang, G. Liu, B. Zheng, H. Yang, J. Sun, X. Xi, and H.-H. Wen, Absence of near-ambient superconductivity in  $\text{LuH}_{2\pm x}\text{N}_y$ , *Nature (London)* **620**, 72 (2023).
- [15] X. Xing, C. Wang, L. Yu, J. Xu, C. Zhang, M. Zhang, S. Huang, X. Zhang, B. Yang, X. Chen, Y. Zhang, J. Guo, Z. Shi, Y. Ma, C. Chen, and X. Liu, Observation of non-superconducting phase changes in  $\text{LuH}_{2\pm x}\text{N}_y$ , *Nat. Commun.* **14**, 5991 (2023).
- [16] Y.-J. Zhang, X. Ming, Q. Li, X. Zhu, B. Zheng, Y. Liu, C. He, H. Yang, and H.-H. Wen, Pressure induced color change and evolution of metallic behavior in nitrogen-doped lutetium hydride, *Sci. China: Phys. Mech. Astron.* **66**, 287411 (2023).
- [17] K. P. Hilleke, X. Wang, D. Luo, N. Geng, B. Wang, F. Belli, and E. Zurek, Structure, stability, and superconductivity of N-doped lutetium hydrides at kbar pressures, *Phys. Rev. B* **108**, 014511 (2023).
- [18] Y. Sun, J. Lv, Y. Xie, H. Liu, and Y. Ma, Route to a superconducting phase above room temperature in electron-doped hydride compounds under high pressure, *Phys. Rev. Lett.* **123**, 097001 (2019).
- [19] C. Wang, S. Yi, S. Liu, and J. H. Cho, Underlying mechanism of charge transfer in Li-doped  $\text{MgH}_{16}$  at high pressure, *Phys. Rev. B* **102**, 184509 (2020).
- [20] H. Xie, D. Duan, Z. Shao, H. Song, Y. Wang, X. Xiao, D. Li, F. Tian, B. Liu, and T. Cui, High-temperature superconductivity in ternary clathrate  $\text{YCaH}_{12}$  under high pressures, *J. Phys.: Condens. Matter* **31**, 245404 (2019).
- [21] X. Liang, A. Bergara, L. Wang, B. Wen, Z. Zhao, X. F. Zhou, J. He, G. Gao, and Y. Tian, Potential high- $T_c$  superconductivity in  $\text{CaYH}_{12}$  under pressure, *Phys. Rev. B* **99**, 100505(R) (2019).
- [22] Y. K. Wei, L. Q. Jia, Y. Y. Fang, L. J. Wang, Z. X. Qian, J. N. Yuan, G. Selvaraj, G. F. Ji, and D. Q. Wei, Formation and superconducting properties of predicted ternary hydride  $\text{ScYH}_6$  under pressures, *Int. J. Quantum Chem.* **121**, e26459 (2021).
- [23] H. B. Ding, Y. J. Feng, M. J. Jiang, H. L. Tian, G. H. Zhong, C. L. Yang, X. J. Chen, and H. Q. Lin, Ambient-pressure high- $T_c$  superconductivity in doped boron-nitrogen clathrates  $\text{La}(\text{BN})_5$  and  $\text{Y}(\text{BN})_5$ , *Phys. Rev. B* **106**, 104508 (2022).
- [24] Y. Ge, F. Zhang, and R. J. Hemley, Room-temperature superconductivity in boron-and nitrogen-doped lanthanum superhydride, *Phys. Rev. B* **104**, 214505 (2021).
- [25] S. D. Cataldo, W. von der Linden, and L. Boeri, First-principles search of hot superconductivity in La-X-H ternary hydrides, *npj Comput. Mater.* **8**, 2 (2022).
- [26] D. V. Semenov, I. A. Troyan, A. G. Ivanova, A. G. Kvashnin, I. A. Kruglov, M. Hanfland, A. V. Sadakov, O. A. Sobolevskiy, K. S. Pervakov, I. S. Lyubutin, K. V. Glazyrin, N. Giordano, D. N. Karimov, A. L. Vasiliev, R. Akashi, V. M. Pudalov, and A. R. Oganov, Superconductivity at 253 K in lanthanum-yttrium ternary hydrides, *Mater. Today* **48**, 18 (2021).
- [27] S. Cai, J. Guo, H. Shu, L. Yang, P. Wang, Y. Zhou, J. Zhao, J. Han, Q. Wu, W. Yang, T. Xiang, H.-k. Mao, and L. Sun, No evidence of superconductivity in a compressed sample prepared from lutetium foil and  $\text{H}_2/\text{N}_2$  gas mixture, *Matter Radiat. Extremes* **8**, 048001 (2023).
- [28] See Supplemental Material at <http://link.aps.org/supplemental/10.1103/PhysRevB.108.214505> for further details on the sample preparation and further discussion of the trigonal phase and its transformation to the cubic phases. It also includes Refs. [73–81].
- [29] B. Kong, L. Zhang, X.-R. Chen, T.-X. Zeng, and L.-C. Cai, Structural relative stabilities and pressure-induced phase transitions for lanthanide trihydrides  $\text{REH}_3$  (RE=Sm, Gd, Tb, Dy, Ho, Er, Tm, and Lu), *Physica B (Amsterdam)* **407**, 2050 (2012).
- [30] M. Tkacz and T. Palasyuk, Pressure induced phase transformation of  $\text{REH}_3$ , *J. Alloys Compd.* **446–447**, 593 (2007).
- [31] M. Mansmann and W. Wallace, The structure of  $\text{HoD}_3$ , *J. Phys. (Paris)* **25**, 454 (1964).
- [32] Đ. Dangić, P. Garcia-Goiricelaya, Y.-W. Fang, J. Ibañez-Azpiroz, and I. Errea, *Ab initio* study of the structural, vibrational, and optical properties of potential parent structures of nitrogen-doped lutetium hydride, *Phys. Rev. B* **108**, 064517 (2023).
- [33] C.-M. Lin, K.-T. Wu, T.-L. Hung, H.-S. Sheu, M.-H. Tsai, J.-F. Lee, and J.-J. Lee, Phase transitions in under high pressure, *Solid State Commun.* **150**, 1564 (2010).
- [34] S. Jiang, J. Liu, C. Lin, L. Bai, W. Xiao, Y. Zhang, D. Zhang, X. Li, Y. Li, and L. Tang, Pressure-induced phase transition in cubic  $\text{Lu}_2\text{O}_3$ , *J. Appl. Phys.* **108**, 083541 (2010).
- [35] T. Palasyuk and M. Tkacz, Pressure-induced structural phase transition in rare-earth trihydrides. Part I. ( $\text{GdH}_3$ ,  $\text{HoH}_3$ ,  $\text{LuH}_3$ ), *Solid State Commun.* **133**, 481 (2005).
- [36] H. Kierey, M. Rode, A. Jacob, A. Borgschulte, and J. Schoenes, Raman effect and structure of  $\text{YH}_3$  and  $\text{YD}_3$  thin epitaxial films, *Phys. Rev. B* **63**, 134109 (2001).
- [37] W. L. Vos, L. W. Finger, R. J. Hemley, J. Z. Hu, H. K. Mao, and J. A. Schouten, A high-pressure van der Waals compound in solid nitrogen-helium mixtures, *Nature (London)* **358**, 46 (1992).
- [38] M. A. Kuzovnikov, M. Tkacz, H. Meng, D. I. Kapustin, and V. I. Kulakov, High-pressure synthesis of tantalum dihydride, *Phys. Rev. B* **96**, 134120 (2017).
- [39] M. A. Kuzovnikov, V. E. Antonov, A. S. Ivanov, T. Hansen, S. Savvin, V. I. Kulakov, M. Tkacz, and A. I. Kolesnikov, Neutron scattering study of tantalum monohydride and monodeuteride, *Int. J. Hydrogen Energy* **46**, 20630 (2021).
- [40] T. Sato, N. Funamori, and T. Yagi, Helium penetrates into silica glass and reduces its compressibility, *Nat. Commun.* **2**, 345 (2011).
- [41] A. Merlen, N. Bendiab, P. Toulemonde, A. Aouizerat, A. San Miguel, J. L. Sauvajol, G. Montagnac, H. Cardon, and P. Petit, Resonant Raman spectroscopy of single-wall carbon nanotubes under pressure, *Phys. Rev. B* **72**, 035409 (2005).
- [42] A. Merlen, P. Toulemonde, N. Bendiab, A. Aouizerat, J. L. Sauvajol, G. Montagnac, H. Cardon, P. Petit, and A. San Miguel, Raman spectroscopy of open-ended single wall carbon nanotubes under pressure: Effect of the pressure transmitting medium, *Phys. Status Solidi B* **243**, 690 (2006).

- [43] J. E. Schirber, G. H. Kwei, J. D. Jorgensen, R. L. Hitterman, and B. Morosin, Room-temperature compressibility of  $C_{60}$ : Intercalation effects with He, Ne, and Ar, *Phys. Rev. B* **51**, 12014 (1995).
- [44] T. Yagi, E. Iida, H. Hirai, N. Miyajima, T. Kikegawa, and M. Bunno, High-pressure behavior of a  $SiO_2$  clathrate observed by using various pressure media, *Phys. Rev. B* **75**, 174115 (2007).
- [45] M. Gauthier, Ph. Pruzan, J. Besson, G. Hamel, and G. Syfosse, Investigation of the phase diagram of ammonia by Raman scattering, *Physica B+C (Amsterdam)* **139-140**, 218 (1986).
- [46] M. Gauthier, Ph. Pruzan, J. C. Chervin, and J. M. Besson, Raman scattering study of ammonia up to 75 GPa: Evidence for bond symmetrization at 60 GPa, *Phys. Rev. B* **37**, 2102 (1988).
- [47] R. Ouillon, C. Turc, J.-P. Lemaistre, and P. Ranson, High resolution Raman spectroscopy in the  $\alpha$  and  $\beta$  crystalline phases of  $N_2$ , *J. Chem. Phys.* **93**, 3005 (1990).
- [48] S. Buchsbaum, R. L. Mills, and D. Schiferl, Phase diagram of nitrogen determined by Raman spectroscopy from 15 to 300 K at pressures to 52 GPa, *J. Phys. Chem.* **88**, 2522 (1984).
- [49] H. Ohno, Y. Iizuka, and S. Fujita, Pure rotational Raman spectroscopy applied to  $N_2/O_2$  analysis of air bubbles in polar firn, *J. Glaciol.* **67**, 903 (2021).
- [50] S. Ninet, F. Datchi, A. M. Saitta, M. Lazzeri, and B. Canny, Raman spectrum of ammonia IV, *Phys. Rev. B* **74**, 104101 (2006).
- [51] T. Suehiro, N. Hirotsuki, Y. Yamamoto, T. Nishimura, M. Mitomo, J. Takahashi, and H. Yamane, Preparation of lutetium nitride by direct nitridation, *J. Mater. Res.* **19**, 959 (2004).
- [52] S. Granville, C. Meyer, A. R. H. Preston, B. M. Ludbrook, B. J. Ruck, H. J. Trodahl, T. R. Paudel, and W. R. L. Lambrecht, Vibrational properties of rare-earth nitrides: Raman spectra and theory, *Phys. Rev. B* **79**, 054301 (2009).
- [53] S. K. Singh and U. P. Verma, Investigation of high pressure phase transition and electronic properties of lutetium nitride, *J. Phys.: Conf. Ser.* **640**, 012029 (2015).
- [54] S. S. Chouhan, G. Pagare, P. Soni, S. P. Sanyal, A. B. Garg, R. Mittal, and R. Mukhopadhyay, High pressure phase transition and elastic properties of lutetium mononitrides, in *Solid State Physics: Proceedings of the 55th DAE Solid State Physics Symposium 2010, Manipal University, Manipal, India, 26–30 December 2010* (American Institute of Physics, Melville, NY, 2011), pp. 97–98.
- [55] K. Niwa, M. Hasegawa, and T. Yagi, Synthesis of Ln nitrides (Ln=Ce, Pr, Gd, Lu) in high pressure and temperature, *J. Alloys Compd.* **477**, 493 (2009).
- [56] R. Lucrezi, P. P. Ferreira, M. Aichhorn, and C. Heil, Temperature and quantum anharmonic lattice effects in lutetium trihydride: Stability and superconductivity, [arXiv:2304.06685](https://arxiv.org/abs/2304.06685).
- [57] J. N. Daou and J. Bonnet, Étude de la résistivité des phases solides du système lutétium-hydrogène, *C. R. Hebd. Seances Acad. Sci.* **261**, 1675 (1965).
- [58] P. Subramanian and J. Smith, Hydrogen vapor pressure measurements over a portion of the Lu-H system, *J. Less-Common Met.* **87**, 205 (1982).
- [59] J. Bonnet, The effect of hydrogen solution on the anisotropy of the crystalline properties of rare-earth metals, *J. Less-Common Met.* **49**, 451 (1976).
- [60] J. Daou and J. Bonnet, A new behaviour of the interstitial element H or D in solution in rare-earth metal, *J. Phys. Chem. Solids* **35**, 59 (1974).
- [61] J. Yang and L. An, Elasticity, ideal tensile strength and lattice dynamics of  $LuH_2$  dihydride from first-principles investigations, *Int. J. Hydrogen Energy* **41**, 2720 (2016).
- [62] J. E. Bonnet and J. N. Daou, Rare-earth dihydride compounds: Lattice thermal expansion and investigation of the thermal dissociation, *J. Appl. Phys.* **48**, 964 (1977).
- [63] S.-W. Kim, L. J. Conway, C. J. Pickard, G. L. Pascut, and B. Monserrat, Microscopic theory of colour in lutetium hydride *Nat. Commun.* **14**, 7360 (2023).
- [64] Q. Luo, C. Lu, L. Liu, and M. Zhu, A review on the synthesis of transition metal nitride nanostructures and their energy related applications, *Green Energy Environ.* **8**, 406 (2023).
- [65] T. Dierkes, J. Plewa, and T. Jüstel, From metals to nitrides - Syntheses and reaction details of binary rare earth systems, *J. Alloys Compd.* **693**, 291 (2017).
- [66] P. P. Ferreira, L. J. Conway, A. Cucciari, S. Di Cataldo, F. Giannessi, E. Kogler, L. T. F. Eleno, C. J. Pickard, C. Heil, and L. Boeri, Search for ambient superconductivity in the Lu-N-H system, *Nat. Commun.* **14**, 5367 (2023).
- [67] R. Dias, High temperature and low pressure superconductor, World Intellectual Property Organization Publication No. WO/2023/064019, International Application No. PCT/US2022/038408 (2023).
- [68] T. Kume, H. Ohura, S. Sasaki, H. Shimizu, A. Ohmura, A. Machida, T. Watanuki, K. Aoki, and K. Takemura, High-pressure study of  $YH_3$  by Raman and visible absorption spectroscopy, *Phys. Rev. B* **76**, 024107 (2007).
- [69] Y. Yao and D. D. Klug, Consecutive Peierls distortions and high-pressure phase transitions in  $YH_3$ , *Phys. Rev. B* **81**, 140104(R) (2010).
- [70] T. Kume, H. Ohura, T. Takeichi, A. Ohmura, A. Machida, T. Watanuki, K. Aoki, S. Sasaki, H. Shimizu, and K. Takemura, High-pressure study of  $ScH_3$ : Raman, infrared, and visible absorption spectroscopy, *Phys. Rev. B* **84**, 064132 (2011).
- [71] D. Peng, Q. Zeng, F. Lan, Z. Xing, Y. Ding, and H.-k. Mao, The near-room-temperature upsurge of electrical resistivity in Lu-H-N is not superconductivity, but a metal-to-poor-conductor transition, *Matter Radiat. Extremes* **8**, 058401 (2023).
- [72] N. P. Salke, A. C. Mark, M. Ahart, and R. J. Hemley, Evidence for near ambient superconductivity in the Lu-N-H system, [arXiv:2306.06301](https://arxiv.org/abs/2306.06301) [cond-mat.supr-con].
- [73] A. Pebler and W. E. Wallace, Crystal structures of some lanthanide hydrides, *J. Phys. Chem.* **66**, 148 (1962).
- [74] J. Rodríguez-Carvajal, Recent advances in magnetic structure determination by neutron powder diffraction, *Physica B (Amsterdam)* **192**, 55 (1993).
- [75] C. Prescher and V. B. Prakapenka, *DIOPTAS*: A program for reduction of two-dimensional x-ray diffraction data and data exploration, *High Pressure Res.* **35**, 223 (2015).
- [76] B. H. Toby and R. B. Von Dreele, *GSAS-II*: The genesis of a modern open-source all purpose crystallography software package, *J. Appl. Crystallogr.* **46**, 544 (2013).
- [77] S. Klotz, J.-C. Chervin, P. Munsch, and G. Le Marchand, Hydrostatic limits of 11 pressure transmitting media, *J. Phys. D: Appl. Phys.* **42**, 075413 (2009).

- [78] J. Bonnet and J. N. Daou, Étude radiocristallographique de la phase alpha du système lutétium-hydrogène entre 25 et 540°C. Coefficients moyens d'expansion thermique, *C. R. Seances Acad. Sci. Ser. C* **272**, 1697 (1971).
- [79] M. I. Eremets and I. A. Troyan, Conductive dense hydrogen, *Nat. Mater.* **10**, 927 (2011).
- [80] M. I. Eremets, V. S. Minkov, P. P. Kong, A. P. Drozdov, S. Chariton, and V. B. Prakapenka, Universal diamond edge Raman scale to 0.5 terapascal and implications for the metallization of hydrogen, *Nat. Commun.* **14**, 907 (2023).
- [81] S. K. Sharma, H. K. Mao, and P. M. Bell, Raman measurements of hydrogen in the pressure range 0.2–630 kbar at room temperature, *Phys. Rev. Lett.* **44**, 886 (1980).